J Physiol 594.12 (2016) pp 3353–3370

The Journal of Physiology

Lysosomal cystine accumulation promotes mitochondrial depolarization and induction of redox-sensitive genes in human kidney proximal tubular cells

Rodolfo Sumayao[1], Bernadette McEvoy[1], Philip Newsholme[2] and Tara McMorrow[1]

[1] *Conway Institute, School of Biomolecular and Biomedical Science, University College Dublin, Dublin, Ireland*
[2] *School of Biomedical Sciences, CHIRI Biosciences Research Precinct and Faculty of Health Sciences, Curtin University, Perth, Western Australia*

Key points

- Cystine is a disulphide amino acid that is normally generated in the lysosomes by the breakdown of cystine-containing proteins.
- Previously, we demonstrated that lysosomal cystine accumulation in kidney proximal tubular epithelial cells (PTECs) dramatically reduced glutathione (GSH) levels, which may result in the disruption of cellular redox balance.
- In the present study, we show that lysosomal cystine accumulation following CTNS gene silencing in kidney PTECs resulted in elevated intracellular reactive oxygen species production, reduced antioxidant capacity, induction of redox-sensitive proteins, altered mitochondrial integrity and augmented cell death.
- These alterations may represent different facets of a unique cascade leading to tubular dysfunction initiated by lysosomal cystine accumulation and may present a clear disadvantage for cystinotic PTECs *in vivo*.
- Cystine depletion by cysteamine afforded cytoprotection in CTNS knockdown cells by reducing oxidative stress, normalizing intracellular GSH and ATP content, and preserving cell viability.

Abstract Cystine is a disulphide amino acid that is normally generated within the lysosomes through lysosomal-based protein degradation and via extracellular uptake of free cystine. In the autosomal recessive disorder, cystinosis, a defect in the CTNS gene results in excessive lysosomal accumulation of cystine, with early kidney failure a hallmark of the disease. Previously, we demonstrated that silencing of the CTNS gene in kidney proximal tubular epithelial cells (PTECs) resulted in an increase in intracellular cystine concentration coupled with a dramatic reduction in the total GSH content. Because of the crucial role of GSH in maintaining the redox status and viability of kidney PTECs, we assessed the effects of CTNS knockdown-induced lysosomal cystine accumulation on intracellular reactive oxygen species (ROS) production, activity of classical redox-sensitive genes, mitochondrial integrity and cell viability. Our results showed that lysosomal cystine accumulation increased ROS production and solicitation to oxidative stress (OS). This was associated with the induction of classical redox-sensitive proteins, NF-κB, NRF2, HSP32 and HSP70. Cystine-loaded PTECs also displayed depolarized mitochondria, reduced ATP content and augmented apoptosis. Treatment of CTNS knockdown PTECs with the cystine-depleting agent cysteamine resulted in the normalization of OS index, increased GSH and ATP content, and preservation of cell viability. Taken together, the alterations observed in cystinotic cells may represent different facets of a cascade leading to tubular dysfunction and, in combination with cysteamine therapy, may offer a novel link for the attenuation of renal injury and preservation of functions of other organs affected in cystinosis.

DOI: 10.1113/JP271858

(Resubmitted 8 November 2015; accepted after revision 2 February 2016; first published online 24 February 2016)
Corresponding authors T. McMorrow: Conway Institute, School of Biomolecular and Biomedical Science, University College Dublin, Dublin, Ireland. Email: tara.mcmorrow@ucd.ie; P. Newsholme: School of Biomedical Sciences, CHIRI Biosciences Research Precinct and Faculty of Health Sciences, Curtin University, Perth, Western Australia. Email: philip.newsholme@curtin.edu.au

Abbreviations carboxy-H_2DFFDA, 5-(and-6)-carboxy-2′,7′-difluorodihydrofluorescein diacetate; DAF-FMDA, 4-amino-5-methylamino-2′,7′-difluoroflurescein diacetate; DHE, dihyroethidine; ER, endoplasmic reticulum; GSH, glutathione; HSE, heat shock element; HSF-1, heat shock factor-1; HSP, heat shock protein; iNOS, inducible nitric oxide synthase; NF-κB, nuclear factor kappa-light-chain-enhancer of activated B cells; NOX, NADPH oxidase; NRF2, nuclear factor erythroid 2-related factor 2; OS, oxidative stress; PI, propidium iodide; PS, propidium iodide; PTEC, proximal tubular epithelial cell; RFU, relative fluorescence units; ROS, reactive oxygen species.

Introduction

Cystine is a disulphide amino acid that is normally generated inside the lysosomes by a cathepsin-catalysed breakdown of cystine-containing proteins (Thoene & Lemons, 1980). However, experimental data on cystinotic leukocytes and fibroblasts have shown that part of the lysosomal cystine pool originates from the uptake of extracellular non-protein cystine (Schulman *et al.* 1969; Danpure *et al.* 1986). In renal proximal tubules, most of this non-protein cystine uptake is mediated by the apical heterodimertic transporter, $b^{0,+}$AT-RBAT, encoded by the *$b^{0,+}$AT1/SLC7A9* and *rBAT/SLC3A1* genes (Pras *et al.* 1995; Feliubadaló *et al.* 1999). Although the extent to which the apical uptake of cystine *versus* the hydrolysis of reabsorbed proteins contributes to proximal tubular cystine pool has not yet been fully established, the cystine compartmentalized in the lysosome represents > 90% of the intracellular cystine pool (Gahl *et al.* 1982; Ghal *et al.*, 1982).

In the autosomal recessive disorder cystinosis, cystine accumulates at greatly elevated levels in the lysosomes of the cell (Gahl, 2001; Gahl *et al.* 2002). Although the widespread lysosomal accumulation of cystine in different tissues leads to multi-organ dysfunction, the loss of kidney function remains the foremost clinical characteristic of this disease. The cystinosis-associated kidney dysfunction is clinically manifested by the excessive loss of water, electrolytes, minerals and essential nutrients into the urine, a condition known as Fanconi syndrome (Gahl, 2001; Gahl *et al.* 2002). The disease is caused by one or more mutations in the CTNS gene, which codes for a lysosomal transmembrane protein, cystinosin (Town *et al.* 1998; Gahl, 2001; Gahl *et al.* 2002). Cystinosin is a 367 amino acid cystine/H^+ symporter whose only known function, to date, is to facilitate the efflux of cystine from the lysosomal compartment to the cytosol (Kalatzis *et al.* 2001), where it is subsequently reduced to cysteine by cytosolic reducing systems (Wilmer *et al.* 2010*a*).

It has been reported that the expression of cystinosin is particularly robust in the renal proximal tubules compared with other segments of the nephron (Kalatzis *et al.* 2004), suggesting that cystinosin is essential for proximal tubular cell function. Theoretically, sequestration of cystine in the lysosomes, a consequence of defective cystinosin, may result in the cytosolic deficit in cysteine, which is the primary limiting factor for the synthesis of the main intracellular antioxidant glutathione (GSH). Because GSH is essential for the tight control and modulation of cellular redox status, it is tempting to speculate that sequestration of cystine within the lysosomal compartment may result in the perturbation of redox status which, in turn, can lead to the activation of redox-sensitive signalling pathways. These signalling pathways can induce the expression of genes whose protein products can either confer cytoprotection or lead to inappropriate cell death. Furthermore, a deficiency in GSH can result in increased concentration of reactive oxygen species (ROS), which can indiscriminately target mitochondrial proteins, significantly impacting energy generating capacity. In this study, the effects of lysosomal cystine accumulation, associated with CTNS gene inhibition, on intracellular redox status were extensively investigated in kidney proximal tubular epithelial cells (PTECs). The impact of these redox alterations on oxidative damage, ROS generation, mitochondrial integrity and cell viability was assessed. Because loss of cystinosin function can elicit a stress response via redox-sensitive transcription factors, we attempted to gain further insights into the influence of lysosomal cystine accumulation on the expression of some classical stress-responsive proteins. The effects of the cystine-depleting drug cysteamine on rescuing the cellular phenotypes associated with lysosomal cystine accumulation were also investigated.

Methods

Cell culture

HK-2 cells, a PTEC line derived from a normal adult human kidney, were cultured as described previously (Sumayao *et al.* 2013). Unless otherwise stated, all reagents were purchased from Sigma-Aldrich (St Louis, MO, USA).

siRNA transfection and assessment of CTNS knockdown

The selection and production of CTNS-targeting siRNAs (siCTNS), based on the human CTNS gene sequence, were performed by Dharmacon, Inc. (Lafayette, CO, USA) using the SMARTpool technology, which combines four highly potent siRNAs to mimic the natural silencing pathway. A non-targeting siRNA (siNT) pool designed to target no known genes in human was supplied by the same vendor as a negative control. HK-2 cells were cultured in antibiotic- and serum-free medium to obtain ∼40% confluence. siRNA transfection was performed as described previously (Sumayao *et al.* 2013). The assessment of CTNS gene silencing and intracellular cystine accumulation was also described in Sumayao *et al.* (2013). Succeeding experiments were performed 72 h following transfection.

Intracellular ROS levels and OS index

Intracellular superoxide (O_2^-) and NO levels were determined in live cells using dihyroethidine (DHE) and 4-amino-5-methylamino-2′,7′-difluoroflurescein diacetate (DAF-FMDA), respectively. DHE is a redox-sensitive probe which is oxidized by O_2^- to form a fluorescent product, 2-hydroxyethidium (2-OH-E^+) and ethidium (E^+) (Zhao *et al.* 2003). DAF-FMDA is a cell-permeant probe which is deacetylated by intracellular esterases/deacetylases to become DAF-FM. The fluorescence of DAF-FM increases 160-fold after reacting with NO (Kojima *et al.* 1999). The OS index of cells was assessed using the probe 5-(and-6)-carboxy-2′,7′-difluorodihydrofluorescein diacetate (carboxy-H_2DFFDA) which is non-fluorescent until the acetate group is removed by intracellular esterases and oxidation occurs within the cell. The oxidation of carboxy-H_2DFFDA not only depends on the intracellular ROS levels but also on the concentration of intracellular antioxidants such as GSH, and hence can be interpreted as an OS index rather than direct evidence of augmented ROS production (Jakubowski & Bartosz, 2000).

For live imaging experiments, cells were seeded in 35 mm uncoated glass-bottom dishes (MatTek Corp., Ashland, MA, USA). The cells were incubated with 5 μM DHE (Invitrogen, Carlsbad, CA, USA) for 30 min, 5 μM DAF-FMDA (Invitrogen) for 45 min or 20 μM carboxy-H_2DFFDA (Invitrogen) for 45 min at 37°C. The cells were washed three times with PBS to remove excess probe and incubated with serum-free medium for 30 min to allow complete de-esterification of intracellular diacetates. The fluorescence emission of the oxidized probes was analysed immediately by fluorescence microscopy (Nikon Instruments, Melville, NY, USA). Images were acquired using a computer-controlled Zeiss HRc charge-coupled device (CCD) camera (Carl Zeiss Microscopy GmbH, Jena, Germany) with at least five fields of view collected for each well. Images were analysed using the cell^A Image Acquisition Software (Olympus, Tokyo, Japan).

For flow cytometry experiments, the cells were seeded and grown to 40–50% confluence in six-well tissue culture plates. Following siRNA transfection, dye loading was performed following the procedures described previously. The cells were then washed three times with PBS and gently detached with 0.05% trypsin-EDTA. Trypsin was neutralized by adding culture medium containing 10% fetal calf serum (FCS) to the cell suspension. The cell suspensions were centrifuged at 800 *g* for 3 min, resuspended in PBS and analysed immediately using a BD Accuri C6 cytometer (BD Biosciences, San Jose, CA, USA). Data were analysed using the CFlow Software (BD Biosciences).

Nitrotyrosine content

After siRNA transfection, cells were washed three times with ice-cold PBS and lysed with 25 mM Hepes buffer (pH 7.5) which contained 1% NP-40, 150 mM NaCl, 10 mM $MgCl_2$, 1 mM EDTA and 2% glycerol. The lysates were homogenized using a motorized Teflon pestle for 3 min with vortexing every 30 s. The lysates were centrifuged at 14,000 *g* for 15 min at 4°C. Nitrotyrosine levels in the supernatants were determined by Western blot using an anti-nitrotyrosine antibody (Cell Signaling, Danvers, MA, USA) following the procedures described in the Western blot section.

Additionally, the nitrotyrosine content was determined by a competitive enzyme-linked immunosorbent assay (ELISA) using the OxiSelect Nitrotyrosine ELISA kit (Cell Biolabs, San Diego, CA, USA), according to the instructions of the manufacturer. The nitrotyrosine content was normalized for protein concentration of the supernatant.

Intracellular calcium concentration

Intracellular calcium Ca^{2+} concentration was assessed using the Ca^{2+}-sensitive probe Fluo-4 AM. For live cell imaging experiments, cells were seeded and grown to 40–50% confluence in 35 mm uncoated glass-bottom dishes (MatTek). Following siRNA transfection, cells were washed three times with PBS and incubated with 1 μM Fluo-4 AM (Invitrogen) in serum-free medium at 37°C for 1 h. The cells were washed three times with PBS to remove excess probe and incubated with serum-free medium for 30 min to allow complete de-esterification of intracellular AM esters. The fluorescence emission of Ca^{2+}-bound Fluo-4 was analysed immediately by fluorescence microscopy (Nikon Instruments) as previously described

in the 'Intracellular ROS and OS index' section. Images were analysed using the cell^A Image Acquisition Software (Olympus).

For the flow cytometry measurement of intracellular Ca^{2+} levels, cells were seeded and grown to 40–50% confluence in six-well tissue culture plates. Following siRNA transfection, the cells were loaded with Fluo-4 AM as described previously. The cell suspensions were prepared following the procedures described in the 'Intracellular ROS and OS index' section. The fluorescence emission of the Ca^{2+}-bound Fluo-4 was analysed immediately using a BD Accuri C6 cytometer (BD Biosciences). Data were analysed using the CFlow Software (BD Biosciences).

Mitochondrial transmembrane potential ($\Delta\Psi_m$)

$\Delta\Psi_m$ was assessed using the lipophilic cationic dye JC-1. JC-1 selectively enters the mitochondria and, at high mitochondrial $\Delta\Psi_m$, it spontaneously forms complexes known as J-aggregates, which emit an intense red fluorescence. At low mitochondrial $\Delta\Psi_m$, JC-1 remains in the monomeric form, which shows only green fluorescence.

In brief, cells were washed three times with PBS and incubated with 0.05% trypsin-EDTA solution to facilitate cell dispersal. Trypsin action was terminated by adding culture medium containing 10% FCS to the cell suspension. The cell suspensions were centrifuged at 800 *g* for 3 min at room temperature and the cell pellets were resuspended with 2 μM JC-1 dye (Invitrogen) in serum-free complete culture medium for 30 min at 37°C. Following centrifugation, the cells were resuspended in PBS and were analysed immediately using a BD Accuri C6 cytometer (BD Biosciences). The ratio of J-aggregates to monomers was used to assess mitochondrial $\Delta\Psi_m$.

GSH content

Total intracellular GSH content was determined by an enzyme-recycling method as previously described (Baker *et al.* 1990). The assay is based on the reaction of GSH with 5,5′-dithio-bis-2-nitrobenzoic acid (DTNB) which produces the TNB chromophore with a maximal absorbance at 412 nm. In brief, 10 μl of cell lysates was placed into a 96-well clear-bottom microplate. Then, 200 μl of freshly prepared reaction mixture [0.1 M potassium phosphate buffer (pH 7.5), 1 mM DTNB, 1 mM NADPH and 1 U ml^{-1} GSH reductase] was delivered in each sample. The absorbance of the samples was measured at 412 nm, with 30 s read intervals for 5 min using a scanning microplate reader equipped with a kinetic trace (Molecular Devices, Sunnyvale, CA, USA). The GSH content of the samples was calculated using a standard curve prepared from GSH of known concentrations (0–0.28 mM). GSH concentrations were normalized for the protein content of the samples.

ATP content

The preparation of cell suspensions for ATP assay was performed as previously described (Sumayao *et al.* 2013). Intracellular ATP content was measured using the ATP Bioluminescence Assay Kit HSII (Roche Diagnostics, Mannheim, Germany) following the instructions of the manufacturer. ATP concentrations were normalized for the protein content of cell lysates.

Preparation of protein extracts for Western blot

Cells were washed three times with ice-cold PBS and lysed in 1× radioimmunoprecipitation assay (RIPA) buffer which contained 5 mM EDTA, 1 mM phenylmethylsulfonylfluoride (PMSF), 5 mM sodium fluoride (NaF), 1 mM sodium orthovanadate (Na_3VO_4), protease inhibitor cocktail (1:100) and 1× solution of PhosSTOP phosphatase inhibitor cocktail (Millipore, Billerica, MA, USA). The cell lysates were homogenized by frequent vortexing for 15 min and centrifuged at 14,000 *g* for 15 min at 4°C. The supernatants were collected and stored at −80ºC until analysis.

Western blot

Western blot analysis was performed following the procedures described previously (Sumayao *et al.* 2013). The following concentrations of primary antibodies in 5% non-fat milk/Tris-base saline buffer (pH 7.4) containing 0.1% Tween-20 (TBST) were used: anti-nitrotyrosine (1:2000; Cell Signaling), anti-iNOS (1:1000; Sigma), anti-p47(phox) (1:1000; Cell Signaling), anti-NF-κB (p65) (1:1000; Cell Signaling), Phospho-NF-κB (p65) (1:1000; Cell Signaling), anti-Nrf2 (1:1000; Cell Signaling), anti-Hsp32 and -Hsp70 (1:1000; Cell Signaling), anti-Beclin (1:1000; Cell Signaling), anti-LC3 I/II (1:1000; Cell Signaling), β-actin (1:2000; Thermo Scientific, Waltham, MA, USA) and GAPDH (1:2000; Abnova, Walnut, CA, USA). The membranes were incubated with a 1:2000 dilution of horseradish peroxidase-conjugated IgG (Thermo Scientific) in 5% non-fat milk/TBST. The bound secondary antibodies were detected using the Enhanced Chemiluminescence Kit (Thermo Scientific, Rockford, IL, USA) following the instructions of the manufacturer. Bands were developed on autoradiographic films using an automated developer. Densitometry analyses of bands were performed using the ImageJ software (National Institutes of Health, Bethesda, MD, USA).

Apoptosis and necrosis

The levels of apoptosis and necrosis were assessed by Annexin V-FITC and propidium iodide (PI) co-staining, respectively. Annexin V is a Ca^{2+}-dependent phospholipid-binding protein that has a high affinity for phosphatidylserine (PS) (Koopman *et al.* 1994; Vermes *et al.* 1995). In the early stages of apoptosis, the cell loses membrane asymmetry, which results in the translocation of PS to the outer leaflet of the plasma membrane, thereby exposing it to the external cellular environment (Vermes *et al.* 1995). Therefore, binding of Annexin V to externalized PS can indicate the proportion of cells undergoing apoptosis. PI, on the other hand, is an intercalating agent and a fluorescent molecule that has been widely used for the evaluation of necrosis in different experimental models because of its ability to permeate cells with damaged membranes, a hallmark of late apoptosis or necrosis (Riccardi & Nicoletti, 2006).

The preparation of cell suspensions was performed following the same procedures described in the 'Intracellular ROS and OS index' section. Following centrifugation, the cell pellets were resuspended in 500 μl 1× Annexin V binding buffer (BD Biosciences) and dispersed by passing the cell suspension repeatedly through a pipette to produce single cell suspension; 5 μl of Annexin V-FITC (BD Biosciences) and 5 μl of 1 μg ml^{-1} PI (Invitrogen) were added to the cell suspensions. The cell suspensions were incubated for 5 min at room temperature and protected from light. The cell suspensions were analysed immediately using a BD Accuri C6 flow cytometer (BD Biosciences).

Cell viability

Cell viability was assessed by a resazurin reduction assay and WST-1 assay. The resazurin reduction assay uses the metabolic capacity of cells in reducing the indicator dye resazurin to highly fluorescent resorufin. Resazurin is effectively reduced in the mitochondria by NADPH or NADH dehydrogenase, making it useful in assessing mitochondrial metabolic capacity. In brief, 5000 cells per well were plated into a 96-well black, clear-bottom tissue culture plate (Corning, New York, USA) and grown to ∼40% confluence at 37°C in a humidified atmosphere with 5% CO_2. The cells were incubated with 0.005% resazurin at 37°C for 90 min. The fluorescence of resorufin was measured using a scanning fluorescence microplate reader (Molecular Devices, Sunnyvale, CA, USA) with excitation and emission wavelengths set at 530 and 590 nm, respectively.

The WST-1 assay uses the stable tetrazolium salt WST-1, which is cleaved to soluble formazan by a mechanism largely dependent on the glycolytic production of NADPH by viable cells. The amount of formazan formed in the culture medium directly correlates with the number of metabolically active cells in the culture. The same procedures as in the resazurin reduction assay were followed for plating of cells. Ten microlitres of WST-1 reagent (Roche Diagnostics) was added to each well and incubated at 37°C for 60 min. The absorbance of formazan was measured at 450 and 630 nm (test and reference wavelengths, respectively) using a scanning microplate reader (Molecular Devices). The net absorbance was obtained from the difference in absorbance measured at 630 and 450 nm.

Protein concentration

Determination of protein concentration was performed using the BCA Protein Assay Kit (Thermo Scientific) following the manufacturer's instructions.

Statistical analysis

Statistical analysis was performed using GraphPad Prism 6.0 (GraphPad, San Diego, CA, USA). Results were expressed as mean ± standard deviation (SD) of at least three independent experiments. A standard *t*-test was used to test for statistical significance between siCTNS- and siNT-transfected cells. Differences between multiple group means were analysed using ANOVA followed by *post hoc* analysis using Tukey's multiple comparisons test. For the data expressed as percentage or as fraction/fold, the data were first $\log_{10}$-transformed followed by an appropriate parametric test. A P of 0.05% or less was deemed statistically significant.

Results

Assessment of CTNS gene silencing and intracellular cystine accumulation

The gene silencing efficiency of siCTNS transfection into HK-2 cells was reported previously by our group (Sumayao *et al.* 2013). The transfection of CTNS-targeting siRNAs into HK-2 cells resulted in ∼60 and ∼42% knockdown of CTNS mRNA and cystinosin, respectively, as assessed by Western blot and RT-PCR, respectively. The siRNA-mediated knockdown of the CTNS gene was also associated with a ∼70% increase in intracellular cystine content. Furthermore, the cystine levels observed in CTNS knockdown cells were comparable to the levels reported by Bellomo *et al.* (2010), indicating that the cystine storage defect is preserved in our *in vitro* model (Sumayao *et al.* 2013).

Lysosomal cystine accumulation increases intracellular O_2^- and NO production but does not alter basal OS index

To assess if lysosomal cystine accumulation caused alterations in intracellular ROS production and OS index,

cells were probed with ROS-specific and redox-sensitive dyes following CTNS gene knockdown. Live cell fluorescence imaging showed a more pronounced DHE and DAF-FM oxidation in CTNS knockdown cells compared with siNT transfected cells (Fig. 1*A* and *C*, respectively), indicating increased intracellular O_2^- and NO production, respectively. The levels of O_2^- and NO were further analysed using flow cytometry, which provided us with relative quantities of these ROS. Flow cytometry analysis of intracellular O_2^- and NO levels showed an ∼30% increase ($P < 0.05$) (Fig. 1*B*) and ∼35% increase ($P < 0.01$) (Fig. 1*D*) in CTNS knockdown cells, respectively, compared with controls. Interestingly, despite the increased intracellular O_2^- and NO levels, basal OS index was not significantly increased in CTNS knockdown cells, as assessed by fluorescence microscopy (Fig. 1*E*) and flow cytometry (siNT *vs.* siCTNS, $P = 0.1949$, Fig. 1*F*). Interestingly, under oxidizing conditions (200 μM hydrogen peroxide (H_2O_2), CTNS knockdown cells displayed a more pronounced increase in OS index than siNT-transfected cells, as assessed by live fluorescence imaging (Fig. 1*E*) and flow cytometry (siNT *vs.* siCTNS, $P < 0.05$, Fig. 1*F*).

Lysosomal cystine accumulation promotes nitrosative damage under oxidizing conditions

Because increased intracellular levels of O_2^- and NO can lead to the generation of highly oxidizing peroxynitrite ($ONOO^-$) which, in turn, can induce nitrosative damage by nitrating tyrosine residues in proteins, we determined the effect of CTNS knockdown-induced lysosomal cystine accumulation on nitrotyrosine levels. Using Western blot analysis, CTNS knockdown cells displayed an increase in

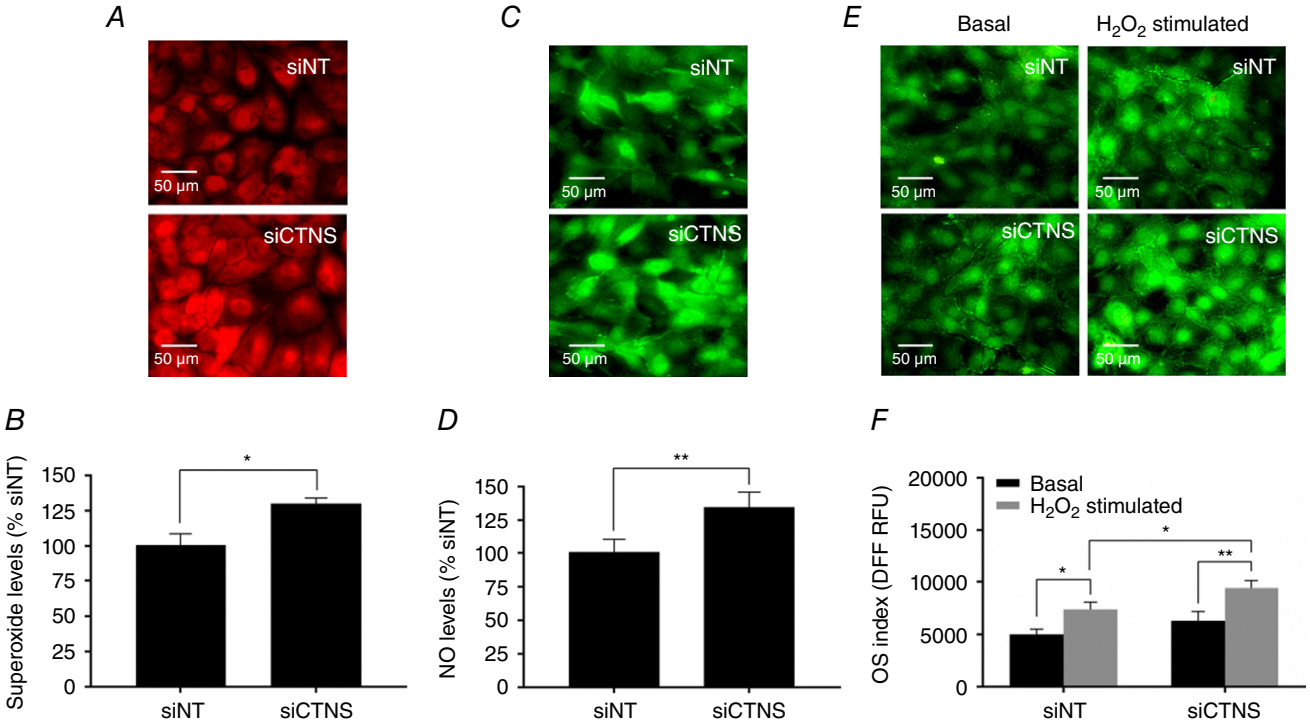

Figure 1. Effect of CTNS knockdown-induced lysosomal cystine accumulation on intracellular ROS level and OS index
HK-2 cells were transfected with CTNS siRNA (siCTNS) pool (50 nM) for 24 h. A separate batch of cells was transfected with a non-targeting siRNA (siNT) pool (50 nM) as a negative control. After 72 h, the intracellular ROS levels and OS index were assessed. Intracellular O_2^- production was monitored in live cells by fluorescence microscopy using a O_2^--sensitive probe DHE. Representative fluorescence images are shown (*A*). Using the same probe, intracellular O_2^- levels were assessed by flow cytometry. O_2^- levels are expressed as mean % siNT ± SD of three independent experiments (*B*). Intracellular NO production was monitored in live cells by fluorescence microscopy using an NO-specific fluorogenic probe, DAF-FMDA. Representative fluorescence images are shown (*C*). Intracellular NO levels were also assessed by flow cytometry using DAF-FMDA. NO levels are expressed as mean % siNT ± SD of three independent experiments (*D*). The general OS index of the cells was assessed by fluorescence microscopy using the redox-sensitive dye DFFDA under basal conditions and in the presence of H_2O_2 (200 μM) for 1 h. Representative fluorescence images are shown (*E*). In a separate experiment, the intracellular oxidation of DFFDA was assessed by flow cytometry. The OS indices are expressed as mean DFF fluorescence (relative fluorescence units, RFU) ± SD of three independent experiments (*F*). Asterisks indicate statistically significant differences at $^*P < 0.01$ and $^{**}P < 0.001$.

nitrotyrosine levels compared with siNT-transfected cells (1.08 *vs.* 1.67 fold change, respectively, $P < 0.05$, Fig. 2*A* and *B*). However, no statistical difference between siNT- and siCTNS-transfected cells was observed when ELISA was used to measure nitrotyrosine levels ($P = 0.3642$, Fig. 2*C*). Under oxidizing conditions, CTNS knockdown cells showed a more pronounced increase in nitrotyrosine levels compared with siNT-transfected cells, as assessed by either Western blot (1.69 *vs.* 2.35 fold change, respectively, $P < 0.05$, Fig. 2*A* and *B*) or ELISA (6.4 *vs.* 8.9 μmol nitrotyrosine mg protein^{-1}, respectively, $P < 0.05$, Fig. 2*B*). The discrepancy observed between Western blot and ELISA may be attributed to the sensitivity of detecting nitrotyrosines associated with these techniques. While ELISA is generally considered more sensitive than Western blot, the prerequisite for most ELISAs is a huge amount of highly purified antigen for optimal detection. The ELISA described in the present study utilized cell lysates which, arguably, might present a limitation for nitrotyrosine detection under basal conditions.

Lysosomal cystine accumulation promotes induction of ROS-generating enzymes

Because iNOS and NOX represent two major sources of cellular ROS in kidney PTECs (Gwinner *et al.* 1998; Beltowski *et al.* 2004; Liu *et al.* 2012), we examined the effect of lysosomal cystine accumulation on the expression of these ROS-generating enzymes by Western blot. The expression of iNOS increased significantly in CTNS knockdown cells by 1.8 ± 0.4-fold ($P < 0.05$) when compared with siNT-transfected cells (Fig. 3*A* and *B*). The expression of p47^{phox}, the cystosolic subunit of NOX, also increased significantly in CTNS knockdown cells by 2.3 ± 0.3-fold ($P < 0.05$) when compared with siNT-transfected cells (Fig. 3*A* and *B*).

Lysosomal cystine accumulation increases intracellular Ca^{2+} flux

Increased intracellular Ca^{2+} flux has been shown to be essential in the activation of NOX via activation of Ca^{2+}-dependent stress kinases, such as protein kinase C (Jiang *et al.* 2011). To determine whether the observed NOX activation in cystine-loaded cells was associated with mobilization intracellular Ca^{2+} stores, the levels of Ca^{2+} in CTNS knockdown cells were assessed using the Ca^{2+}-sensitive fluorogenic probe Fluo-4-AM. Using fluorescence microscopy, CTNS knockdown cells exhibited increased Fluo-4 fluorescence compared with siNT-transfected cells (Fig. 4*A*), indicating increased intracellular Ca^{2+} flux. To validate this observation, intracellular Ca^{2+} levels were further measured by flow cytometry. Consistent with fluorescence microscopy, flow cytometry analysis of Fluo-4 fluorescence showed that

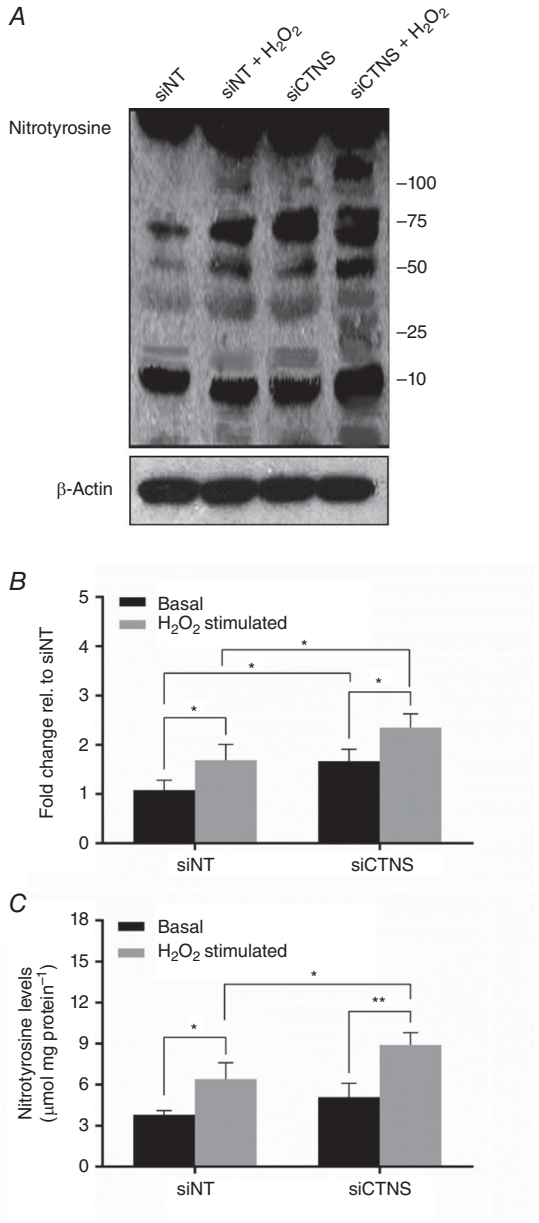

Figure 2. Effect of CTNS knockdown-induced lysosomal cystine accumulation on nitrotyrosine levels
HK-2 cells were transfected with CTNS siRNA pool (siCTNS) for 24 h. A separate batch of cells was transfected with a non-targeting siRNA (siNT) pool (50 nM) as a negative control. Nitrotyrosine levels were assessed 72 h after transfection. Nitrotyrosine levels were determined by Western blot using an anti-nitrotyrosine antibody. A representative blot for nitrotyrosine is shown (*A*). β-Actin was used as a loading control. Densitometry analysis of nitrotyrosine expression was performed by normalizing the band densities of nitrotyrosine for β-actin. Nitrotyrosine levels are expressed as fold change relative (rel) to siNT-transfected cells +/- SD of three independent experiments (*B*). In a separate experiment, nitrotyrosine content was determined by competitive ELISA using an OxiSelect Nitrotyrosine ELISA Kit (Cell Biolabs). Nitrotyrosine levels are expressed as nmol nitrotyrosine mg protein^{-1} ± SD of three independent experiments (*C*). Asterisks indicate statistically significant differences at $^{*}P < 0.01$ and $^{**}P < 0.001$.

CTNS knockdown cells had increased intracellular Ca^{2+} levels compared with siNT-transfected cells [711.6 ± 156.5 *vs.* 1035.0 ± 81.39 relative fluorescence units (RFU), respectively, $P < 0.01$] (Fig. 4*B* and *C*).

Lysosomal cystine accumulation promotes induction redox-sensitive transcription factors and cytoprotective proteins

To gain further insight into the stress responses associated with lysosomal cystine accumulation, we examined the effect of CTNS gene inhibition on the expression of various stress-responsive transcription factors and cytoprotective proteins. One of these transcription factors is NF-κB, which can be activated as a cellular defence mechanism in response to oxidative insult (Flohé *et al.* 1997; Kabe *et al.* 2005). Total NF-κB levels were not significantly different between CTNS- and siNT-transfected cells ($P = 0.19$, Fig. 5*A* and *B*). Interestingly, however, the levels of phosphorylated NF-κB(p65) increased significantly in CTNS knockdown cells compared with siNT-transfected cells (1.6 ± 0.1-fold, $P < 0.05$, Fig. 5*A* and *B*), indicating an augmentation of NF-κB activity.

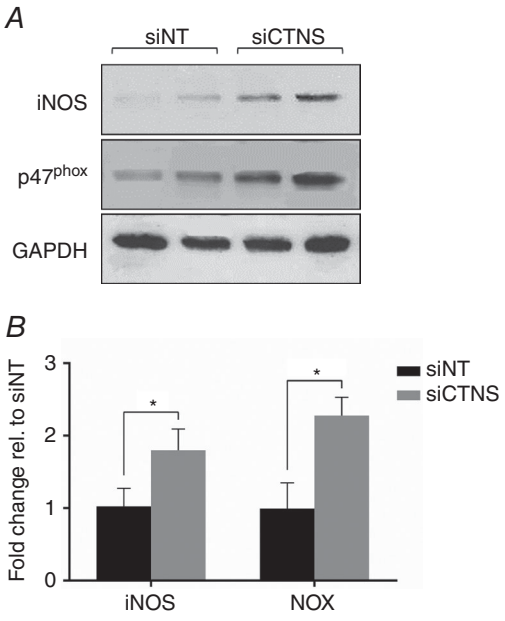

Figure 3. Effect of CTNS knockdown-induced lysosomal cystine accumulation on iNOS and NOX expression
HK-2 cells were transfected with CTNS siRNA pool (siCTNS) for 24 h. A separate batch of cells was transfected with a non-targeting siRNA (siNT) pool (50 nM) as a negative control. iNOS and NOX expression were determined by Western blot 72 h after transfection. Representative blots for iNOS and NOX are shown (*A*). GAPDH was used as a loading control. Densitometry data for iNOS and NOX were normalized for GAPDH expression and are expressed as fold change relative (rel.) to siNT ± SD of three independent experiments (*B*). *Statistically significant difference at $P < 0.05$.

NRF2 represents another important stress-responsive transcription factor especially during OS (Nguyen *et al.* 2009). Interestingly, despite the lack of generalized OS, total NRF2 levels increased markedly by ∼5-fold ($P < 0.05$) under increased lysosomal cystine conditions (Fig. 5*C* and *D*).

Heat shock proteins (HSP) are key proteins that play a cytoprotective role during cellular stress and redox imbalance (Kregel, 2002; Kalmar & Greensmith, 2009). The induction of HSP expression is regulated by the interaction of heat shock factors (HSF) with regulatory elements in DNA termed heat shock elements (HSE) (Kregel, 2002). To assess whether lysosomal cystine accumulation induced heat shock response, we determined the effect of CTNS gene inhibition on the expression of HSF1, HSP70 and HSP32. Total HSF1 levels remained unchanged in CTNS knockdown cells when compared with siNT-transfected cells ($P = 0.3643$, Fig. 5*E* and *F*). While total HSF1 levels were unaffected, both HSP70 and HSP32 increased significantly in CTNS knockdown cells [1.5 ± 0.2-fold ($P < 0.05$) and 1.9 ± 0.4-fold ($P < 0.05$), respectively] (Fig. 5*E* and *F*).

Lysosomal cystine accumulation results in the depolarization of $\Delta\Psi_m$ and in the reduction of intracellular ATP content

Recognizing the crucial role of GSH in preserving mitochondrial integrity, we determined the effects of lysosomal cystine accumulation on $\Delta\Psi_m$. CTNS knockdown cells displayed a significantly increased J-aggregates/J-monomer ratio compared with siNT-transfected cells (2.6 ± 0.3 *vs.* 1.3 ± 0.1, $P < 0.01$, Fig. 6*A* and *B*), indicating depolarization in $\Delta\Psi_m$.

Because the cellular energy status is tightly coupled to mitochondrial integrity, the ATP levels were then measured following CTNS gene silencing. As expected, the ATP levels in CTNS knockdown cells were reduced significantly compared with siNT-transfected cells (1.7 ± 0.3 *vs.* 1.0 ± 0.1 nmol ATP mg protein^{-1}, $P < 0.05$) (Fig. 6*C*).

Lysosomal cystine accumulation does not alter autophagic activity

Mitochondrial autophagy has previously been documented in cystinotic PTECs and has been hypothesized to be an important event leading to ATP depletion (Sansanwal *et al.* 2010*b*). To determine whether similar perturbation in autophagy could be observed in PTECs with reduced CTNS levels, we examined the expression of key autophagy markers in PTECs following CTNS gene inhibition. Interestingly, despite elevated lysosomal cystine load, no alteration in the expression of autophagy markers, Beclin ($P = 0.54$), LC3-I

($P = 0.51$) and LC3-II ($P = 0.07$), was observed in CTNS knockdown cells (Fig. 7*A* and *B*). These data suggest that lysosomal cystine accumulation alone may not be the sole requirement for the induction of autophagy in PTECs and may not be the predominant underlying mechanism leading to ATP depletion observed in CTNS knockdown cells.

Lysosomal cystine accumulation augments apoptosis and reduces cell viability

To assess whether the observed alterations in redox and energy status impacted cell survival, the effects of CTNS knockdown-induced lysosomal cystine accumulation on the levels of apoptosis and necrosis were determined. Since the test described in the present study was an endpoint analysis, it does not distinguish cells that have undergone apoptotic death *versus* those that have died as a result of a necrotic pathway. In general, cells that are in early apoptosis are FITC Annexin V positive and PI negative; cells that are in late apoptosis are both FITC Annexin V and PI positive; cells that are FITC Annexin V negative and PI positive are necrotic cells (Vermes *et al.* 1995). As shown in Fig. 8*A* and *B*, most of the siNT- and siCTNS-transfected cells were in the early apoptotic phase. However, the percentage of early apoptotic cells remained unchanged following CTNS gene knockdown compared with siNT-transfected cells ($P = 0.54$) (Fig. 8*A* and *B*). On the other hand, the percentage of late apoptotic cells increased significantly in CTNS knockdown cells compared with siNT-transfected cells (12.4 ± 1.6 *vs.* $3.1 \pm 1.2\%$, $P < 0.05$) (Fig. 8*A* and *B*). CTNS knockdown

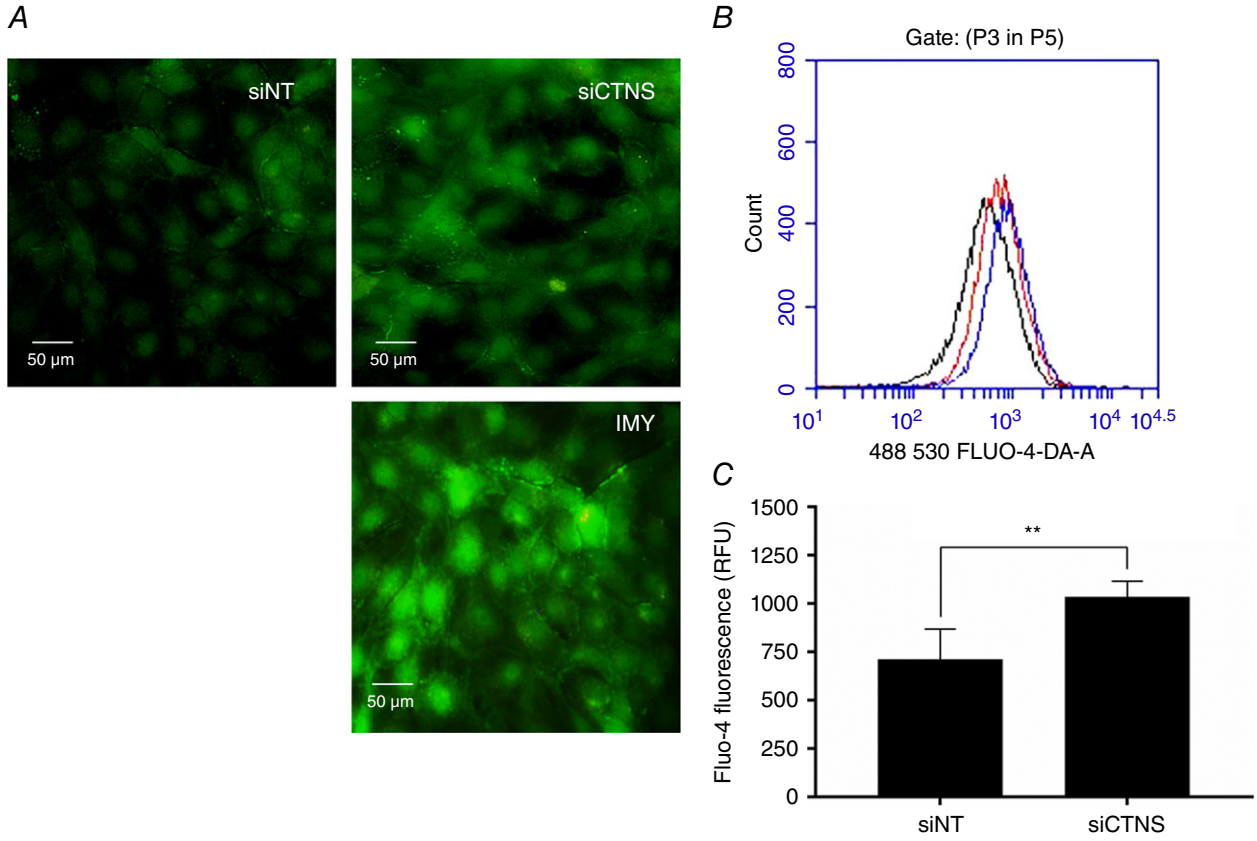

Figure 4. Effect of CTNS knockdown-induced lysosomal cystine accumulation on intracellular Ca^{2+} levels
HK-2 cells were transfected with CTNS siRNA (siCTNS) pool (50 nM) for 24 h. A separate batch of cells was transfected with a non-targeting siRNA (siNT) pool (50 nM) as a negative control. After 72 h, the intracellular Ca^{2+} levels were assessed using the Ca^{2+}-sensitive probe Fluo-4 AM. In one experiment, the fluorescence emission Ca^{2+}-bound Fluo-4 was monitored in live adherent cells by fluorescence microscopy. Representative images are shown (*A*). Using the same probe, intracellular Ca^{2+} levels were quantified in cell suspensions using flow cytometry. A representative single-parameter overlay histogram is shown (*B*) [black curve, siNT; red curve, siCTNS; blue curve, ionomycin (IMY)]. The relative concentration of intracellular Ca^{2+} is expressed as mean Fluo-4 fluorescence (relative fluorescence units, RFU) ± SD of four independent experiments (*C*). IMY (1 mg ml^{-1}), an ionophore that can raise intracellular Ca^{2+} levels, was used as a positive control in both experiments. **Statistically significant difference at $P < 0.01$.

cells also displayed increased necrosis compared with siNT-transfected cells (3.1 ± 0.9 *vs.* $0.96 \pm 0.2\%$, $P < 0.05$) (Fig. 8*A* and *B*).

To further assess the viability of cells under increased lysosomal cystine conditions, we determined the metabolic capacity of the cells in reducing the indicator dyes resazurin and WST-1 to resorufin and formazan, respectively, following CTNS gene knockdown. As shown in Fig. 8*C*, CTNS knockdown cells showed a ~17% reduction ($P < 0.05$) in metabolic capacity in reducing resazurin. Consistent with this observation, CTNS knockdown cells showed a 24% reduction ($P < 0.01$) in metabolic capacity in reducing WST-1 (Fig. 8*C*). These results indicate that the biochemical and metabolic insults initiated by lysosomal cystine accumulation impacted on the viability of kidney PTECs.

Cysteamine treatment reverses some effects associated with lysosomal cystine accumulation

The main treatment for cystinosis is based on lysosomal cystine depletion using the aminothiol, cysteamine. To assess whether cystine depletion can afford protection in cystine-loaded cells, cells were treated with cysteamine following CTNS gene silencing. The optimal cysteamine concentration was first determined by resazurin reduction and WST-1 assay. These experiments established 1000 μM as the optimal cysteamine concentration which consistently resulted to > 90% viability in HK-2 cells following 24 h incubation (results not shown).

We first examined whether cysteamine alone will alter the redox status of cells and, as shown in Fig. 9*A*, cysteamine treatment had no effect on the DFF fluorescence in both siNT- ($P = 0.9999$) and siCTNS-transfected cells ($P = 0.9914$), indicating that cysteamine does not alter the intracellular OS index. To determine the effect of cysteamine on the OS index, cells were incubated with 200 μM H_2O_2 for 1 h to induce OS. As expected, exposure of cells to H_2O_2 increased the OS index in both siNT- (7339.8 ± 858.2 *vs.* 4699.07 ± 592.6 RFU at basal, $P < 0.01$) and siCTNS-transfected cells (9089.8 ± 816.8 *vs.* 5220.3 ± 792.4 RFU at basal, $P < 0.001$) (Fig. 9*A*). However, in the presence of cysteamine, the oxidizing effect of H_2O_2 was blunted in both siNT- (5404.8 ± 629.8, $P < 0.05$) and siCTNS-transfected cells (6275.8 ± 893.7 RFU, $P < 0.01$), suggesting that cysteamine can afford antioxidant protection in kidney PTECs subjected to OS.

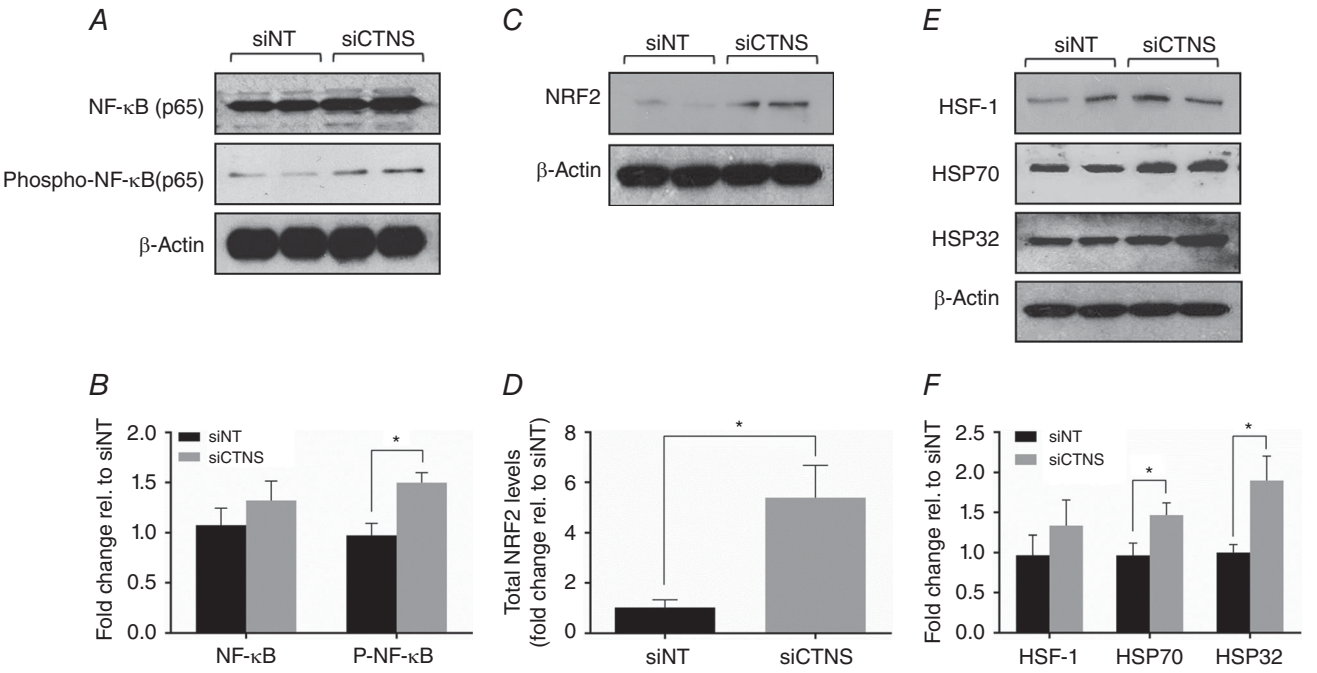

Figure 5. Effect of CTNS knockdown-induced lysosomal cystine accumulation on the expression of stress-responsive proteins
HK-2 cells were transfected with CTNS siRNA (siCTNS) pool (50 nM) for 24 h. A separate batch of cells was transfected with a non-targeting siRNA (siNT) pool (50 nM) as a negative control. The expression of various stress-responsive proteins was determined 72 h after transfection. Representative blots are shown for NF-κB(p65) and phospho-NF-κB(p65) (*A*), NRF2 (*C*), and HSF-1, HSP70 and HSP32 (*E*). β-Actin was used as a loading control in all Western blot experiments. Densitometry analyses of NF-κB(p65) and phospho-NF-κB(p65) (*B*), NRF2 (*D*), and HSF-1, HSP70 and HSP32 (*F*) were performed after normalization for β-actin expression and are expressed as fold-change relative to siNT ± SD of three independent experiments. *Statistically significant difference at $P < 0.05$.

We have previously observed that GSH depletion was one of the biochemical consequences of CTNS knockdown-induced lysosomal cystine accumulation in kidney PTECs (Sumayao *et al.* 2013). Because of the potential of cysteamine as a precursor for cysteine, we examined the effect of cysteamine on GSH levels following CTNS gene knockdown. Not only did cysteamine result in the repletion of intracellular GSH levels, cysteamine treatment markedly increased GSH levels in both siNT- (18.7 ± 3.2 *vs.* 7.9 ± 1.4 nmol GSH mg protein^{-1} at basal, $P < 0.01$) and siCTNS-tranfected cells (23.0 ± 5.0 *vs.* 3.5 ± 0.8 nmol GSH mg protein^{-1} at basal, $P < 0.001$) (Fig. 9*B*). These data indicate that cysteamine, aside from its lysosomal cystine depleting capacity, can promote GSH synthesis in kidney PTECs.

Because GSH is essential for mitochondrial function and integrity to maintain the intracellular energy status, we then investigated whether the GSH boosting effect of cysteamine could also rescue ATP depletion in kidney PTECs with high cystine load. As shown in Fig. 10*A*, cysteamine normalized the ATP levels in CTNS knockdown cells (2.24 ± 0.4 *vs.* 1.30 ± 0.5 nmol ATP mg protein^{-1} at basal, $P < 0.05$), approaching the levels observed in siNT-transfected cells (2.4 ± 0.3 nmol ATP mg protein^{-1}). ATP levels remained unchanged in siNT-transfectd cells following cysteamine treatment

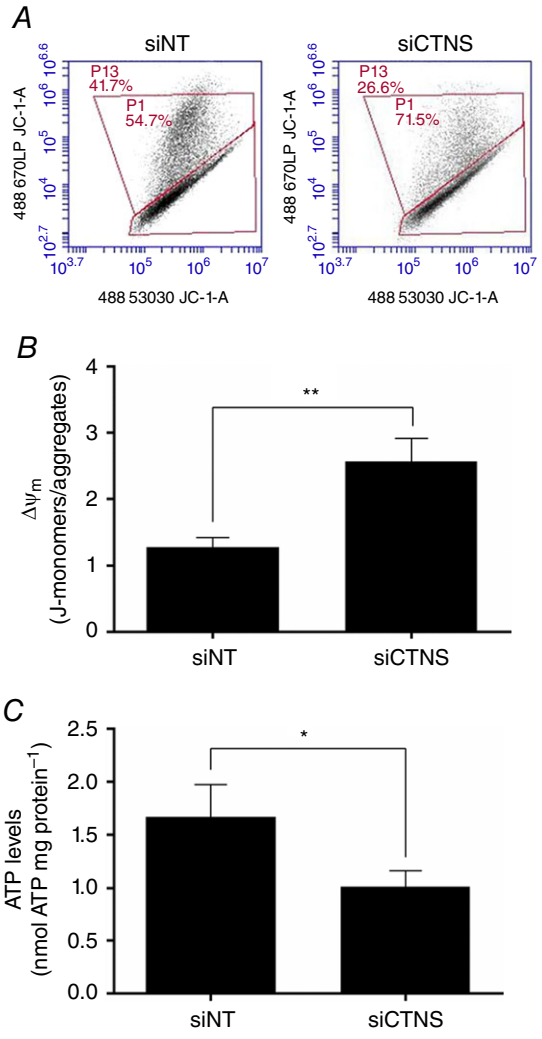

Figure 6. Effect of CTNS knockdown-induced lysosomal cystine accumulation on $\Delta\Psi_m$ and intracellular ATP content
HK-2 cells were transfected with CTNS siRNA (siCTNS) pool (50 nM) for 24 h. A non-targeting siRNA (siNT) pool (50 nM) was used as a negative control. $\Delta\Psi_m$ and intracellular ATP levels were determined 72 h after transfection. $\Delta\Psi_m$ was assessed by flow cytometry using the JC-1 dye. Representative two-dimensional density plots of J-monomers *vs.* J-aggregates are shown (*A*). Flow cytometry data are expressed as the mean ratio of the fluorescence of J-monomers to J-aggregates ± SD of three independent experiments (*B*). Intracellular ATP concentrations were determined using the ATP Bioluminescence Assay Kit HSII (Roche). ATP levels are expressed as mean nmol ATP mg protein^{-1} ± SD of three independent experiments (*C*). Asterisks indicate statistically significant differences at $^{*}P < 0.05$ and $^{**}P < 0.01$.

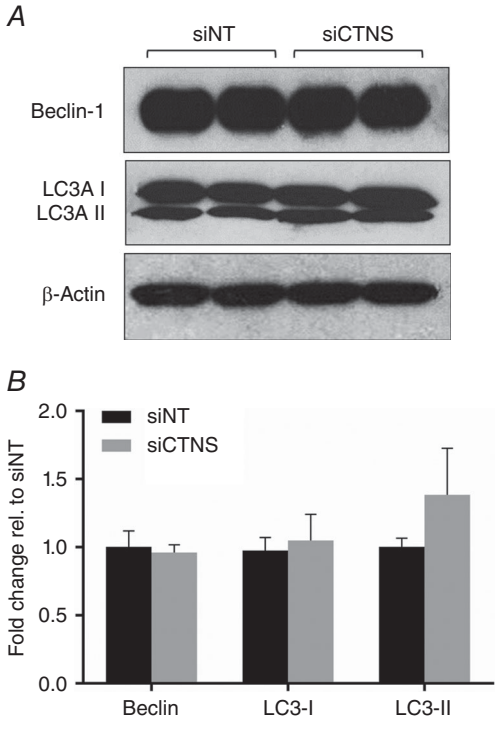

Figure 7. Effect of CTNS knockdown-induced lysosomal cystine accumulation on autophagic activity
HK-2 cells were transfected with CTNS siRNA (siCTNS) pool (50 nM) for 24 h. A separate batch of cells was transfected with a non-targeting siRNA (siNT) pool (50 nM) as a negative control. The expression of various autophagy markers was determined by Western blot 72 h after transfection. Representative blots for Beclin-1, LC3A I and LC3A II are shown (*A*). β-Actin was used as a loading control. Densitometry analyses of Beclin 1, LC3A I and LC3A II expression were performed after normalization for β-actin expression and are expressed as fold-change relative to siNT ± SD of three independent experiments (*B*).

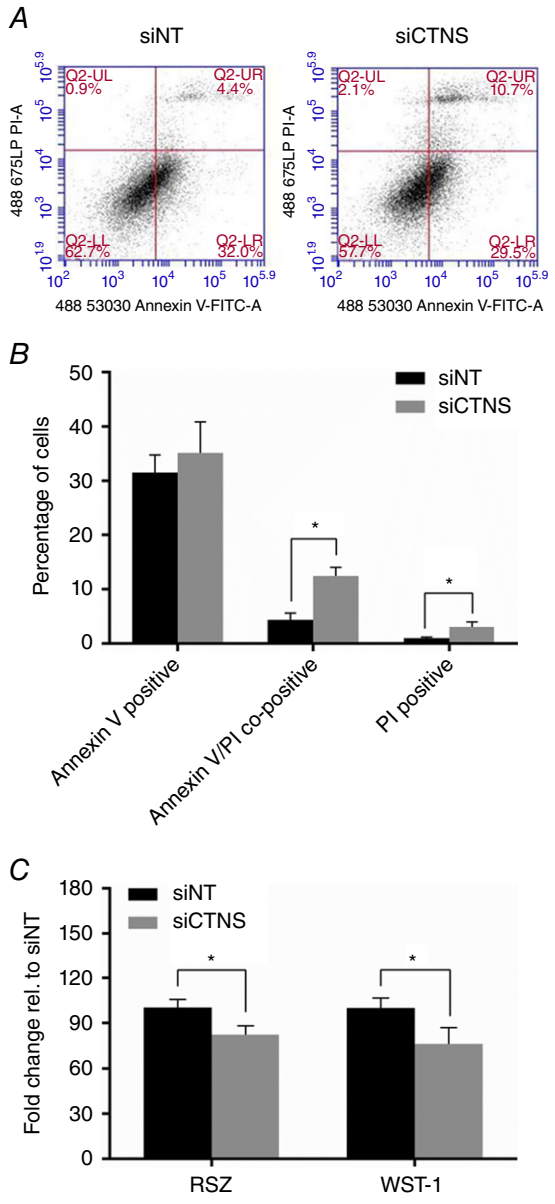

Figure 8. Effect of CTNS knockdown-induced lysosomal cystine accumulation on the levels of apoptosis and necrosis and on cell viability
HK-2 cells were transfected with CTNS siRNA (siCTNS) pool (50 nM) for 24 h. A separate batch of cells was transfected with a non-targeting siRNA (siNT) pool (50 nM) as a negative control. The proportion of apoptotic and necrotic cells were determined by flow cytometry 72 h after transfection using Annexin V-FITC and PI, respectively. Representative two-dimensional plots of Annexin V-FITC (ex: 488 nm; em: 530 ± 30 nm) *vs.* PI (ex: 488 nm; em: 675 nm) are shown (*A*). The levels of early apoptosis, late apoptosis and necrosis are expressed as the percentage of Annexin V-positive, Annexin V/PI-co-positive and PI-positive cells ± SD of three independent experiments, respectively (*B*). Cell viability was determined by assessing the metabolic capacity of cells in reducing the indicator dyes resazurin and WST-1. The resazurin and WST-1 reduction capacity of cells are both expressed as fold-change relative to siNT ± SD of three independent experiments (*C*). *Statistically significant difference at $P < 0.05$.

($P = 0.5268$), suggesting that ATP reduction in CTNS knockdown cells may be, at least in part, a consequence of intracellular GSH depletion.

To determine whether the observed cytoprotective effects mediated by cysteamine could preserve cell viability in kidney PTECs with high cystine load, we determined the effect of cysteamine on the metabolic capacity of cells in reducing resazurin to fluorescent resorufin following CTNS gene knockdown. CTNS knockdown cells displayed increased resorufin fluorescence compared with its matched basal control (3998.8 ± 324.7 *vs.* 2278.6 ± 469.4 RFU, respectively, $P < 0.001$) (Fig. 10*B*) and was comparable to the levels observed in siNT-transfected cells (3181.0 ± 440.7). Interestingly, cysteamine did not further increase the resorufin fluorescence in siNT transfected cells when compared with its matched basal control ($P = 0.1261$). These results indicate that cysteamine treatment promotes preservation of the viability of kidney PTECs under elevated lysosomal cystine conditions, which further substantiates the cytoprotective effect of cysteamine.

Discussion

Early cystinosis research identified lysosomes as the main cystine storage site in cells (Schneider *et al.* 1967*a*; Schulman *et al.* 1969). The physiological and pathological roles of lysosomal cystine accumulation remain poorly understood partly because cystine should not be toxic especially when isolated within the lysosomal compartment, suggesting no obvious disadvantage for cystinotic cells (Park *et al.* 2002). However, it was proposed that lysosomal cystine reserves may possibly be a limiting factor for the synthesis of GSH in the cytosol (Chol *et al.* 2004; Laube *et al.* 2006; Bellomo *et al.* 2010). GSH serves as an important cofactor for the GSH peroxidase family of enzymes, which metabolize H_2O_2 and lipid peroxides, preventing damage to cellular components. Therefore, GSH depletion has become a compelling candidate responsible for the cellular dysfunction associated with cystinosis (Chol *et al.* 2004; Laube *et al.* 2006). Indeed, GSH depletion has been shown to result in mitochondrial dysfunction in several cell and animal models (Han *et al.* 2003). However, GSH deficiency is unlikely to be the sole factor responsible for the complexity of cell stress in cystinosis and this raises the possibility that cells may also respond to other stimuli, which merits further investigation.

We have demonstrated in the present study that CTNS gene inhibition in kidney PTECs was associated with a marked increase in intracellular O_2^- and NO production but did not seem to affect the cells' general OS index. Interestingly, under oxidative challenge induced by H_2O_2, cells with deficient cystinosin displayed a more pronounced increase in OS index, indicating compromised antioxidant capacity. Consistent with our findings, Wilmer

et al. (2011) observed that exposure of conditionally immortalized PTECs obtained from cystinosis patients to high levels of H_2O_2 resulted in more pronounced ROS production compared with healthy cells. Therefore, lysosomal cystine accumulation, as a consequence of lack of cystinosin activity, reduces the capacity of the cell to deal with OS.

Note, however, that the levels of O_2^- and NO represent only one aspect of oxidative stress because these reactive molecules may give rise to a more oxidizing ROS. For example, simultaneous formation of O_2^- and NO produces peroxynitrite ($ONOO^-$), which can induce a more aggressive oxidation, nitrosation, and nitration of biological molecules (Kohen & Nyska, 2002). Uncontrolled production of $ONOO^-$ can indiscriminately target proteins by nitrating tyrosine residues which can adversely affect the function or activity of the protein (Kohen & Nyska, 2002), potentially leading to apoptotic or necrotic cell death. Interestingly, basal levels of nitrotyrosines in CTNS knockdown cells remained normal, suggesting that the antioxidant capacity of these cells may still be sufficient to prevent oxidative damage at basal conditions. However, under oxidizing conditions, CTNS knockdown cells exhibited a more pronounced nitrotyrosination, suggesting increased susceptibility of these cells to oxidative insult.

NOX and iNOS represent major sources of intracellular O_2^- and NO in kidney PTECs, respectively (Beltowski *et al.* 2004; Liu *et al.* 2012). To our knowledge, the present study has provided the first evidence of increased expression of NOX and iNOS in cystinotic-like cells, which may have influenced the observed augmented production of O_2^- and NO in these cells. Although the NOX system may be activated by various cellular stresses, the sequence

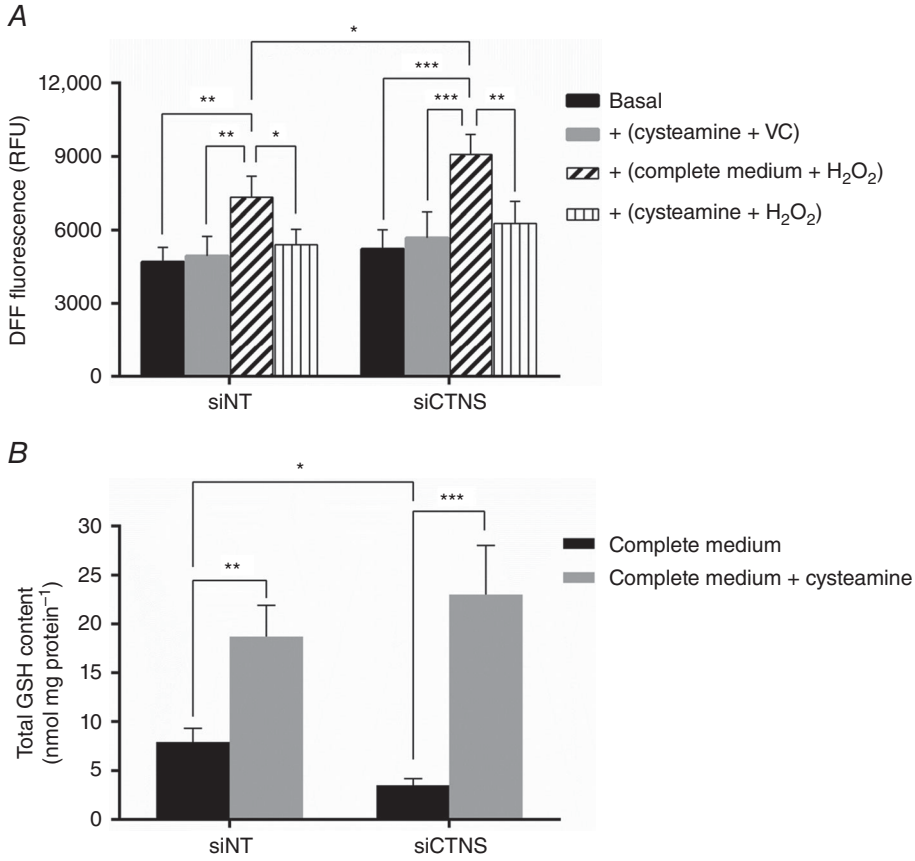

Figure 9. Effect of cysteamine on OS index and intracellular GSH levels
HK-2 cells were transfected with CTNS siRNA (siCTNS) pool (50 nM) for 24 h. A separate batch of cells was transfected with a non-targeting siRNA (siNT) pool (50 nM) as a negative control. After 48 h, the cells were incubated with 1000 μM cysteamine or with complete culture medium for 24 h. Subsequently, 200 μM H_2O_2 or vehicle control was added to the cell culture for 1 h. The OS index was assessed by measuring the fluorescence of the oxidized DFF-DA (i.e. DFF) by flow cytometry. The OS index is expressed as mean DFF fluorescence (relative fluorescence units, RFU) ± SD of four independent experiments (*A*). The effect of cysteamine on the intracellular GSH content was measured by an enzyme recycling assay following incubation of cells with 1000 μM cysteamine or with complete culture medium for 24 h, 48 h after transfection. Total GSH levels are expressed as mean nmol GSH mg protein^{-1} ± SD of four independent experiments (*B*). Asterisks indicate statistically significant differences at $^*P < 0.05$, $^{**}P < 0.01$ and $^{***}P < 0.001$.

of events from lysosomal cystine accumulation leading to NOX induction is largely unknown. One possibility is that altered mitochondrial integrity and subsequent Ca^{2+} release to the cytoplasm may activate Ca^{2+}-dependent stress kinases, such as protein kinase C, which has been shown to be essential in the activation of NOX (Jiang *et al.* 2011). Indeed, we observed a significant increase in the intracellular Ca^{2+} levels in kidney PTECs following CTNS knockdown, a physiological event that may be an upstream signal for the activation of NOX.

NO, if generated at high levels in mitochondria, may result in the auto-oxidation of ubiquinol with concomitant production of O_2^-, H_2O_2, and $ONOO^-$ (Turrens, 2003). These reactive molecules may induce irreversible damage to mitochondrial respiratory complexes and inhibition of ATP synthesis (Turrens, 2003), potentially leading to apoptotic or necrotic cell death. Indeed, we have observed an extensive depolarization of mitochondria and a significant reduction in ATP content following CTNS knockdown, suggesting that mitochondrial integrity and function are compromised under elevated lysosomal cystine conditions. These alterations present a clear disadvantage for cystinotic PTECs *in vivo* as the mass transport of most solutes across the proximal tubular epithelium is largely influenced by the cellular energy (Wilmer *et al.* 2010*a*), which concomitantly supplies some of the essential metabolites to generate energy and preserve redox status. Both ATP and GSH are critical for the survival of kidney PTECs, which are highly metabolically active cells and therefore are constantly exposed to high levels of ROS generated by oxidative mitochondrial metabolism.

Apart from mitochondria, the lysosomes are an important site for ROS production (Nohl & Gille, 2005). It is possible that the elevated ROS and augmented cell death observed in the present study were caused by ROS leakage from the lysosomes. Indeed, lysosomal permeabilization has been proposed to be one of the mechanisms leading to proximal tubular cell death associated with cystinosis (Park *et al.* 2002). Lysosomal permeabilization may be an upstream event leading to ROS leakage, which could then alter the redox status of cells and may lead to inappropriate cell death.

Despite the compendium of studies addressing the role of ATP depletion in the pathogenesis of cystinosis, measurement of ATP levels in cystinotic cells has yielded inconsistent results (Wilmer *et al.* 2005, 2011; Levtchenko *et al.* 2006; Sansanwal *et al.* 2010*b*). It appears that the hypothesis implicating reduced ATP generation as the keystone in the pathogenesis of cystinosis understates the complexity of the problem. Most recently, a striking degree of mitochondrial autophagy and a reduced mitochondrial ATP generation have been observed in cystinotic PTECs, which may be an important event leading to ATP depletion (Sansanwal *et al.* 2010*b*). However, in the present study, the expression of various markers of autophagy was unaltered in CTNS knockdown cells despite increased cystine levels. This observation suggests that cystine accumulation, although regarded

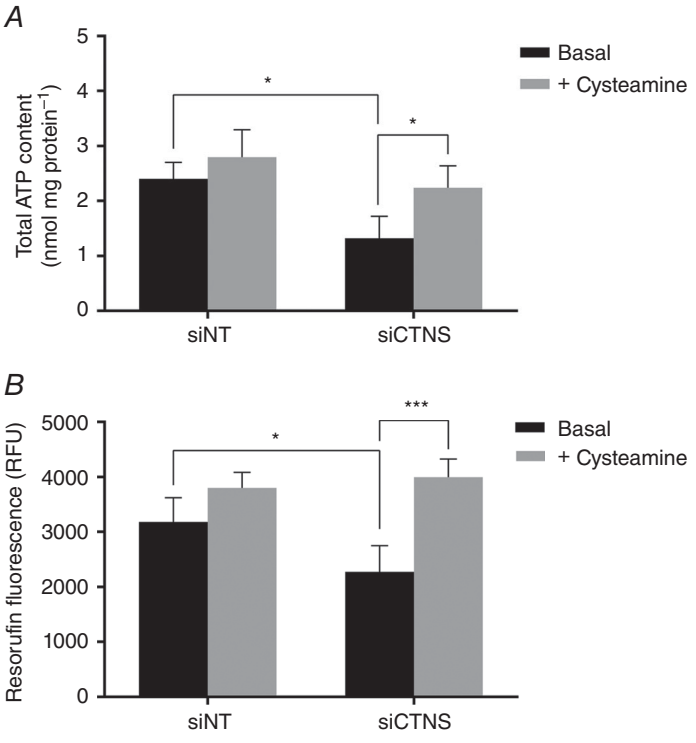

Figure 10. Effect of cysteamine on intracellular ATP content and cell viability
HK-2 cells were transfected with CTNS siRNA (siCTNS) pool (50 nM) for 24 h. As a negative control, a separate batch of cells was transfected with a non-targeting siRNA (siNT) pool (50 nM). After 48 h, the cells were incubated with 1000 μM cysteamine or with complete culture medium for 24 h. Intracellular ATP content was measured using the ATP Bioluminescence Assay Kit HSII (Roche). ATP levels are expressed as mean nmol ATP mg protein^{-1} $\pm$ SD of four independent experiments (*A*). The effect of cysteamine on cell viability was assessed by the metabolic capacity of cells in reducing resazurin to resorufin following incubation of cells with 1000 μM cysteamine or with complete culture medium for 24 h, 48 h after transfection. Cell viability is expressed as mean resorufin fluorescence (relative fluorescence units, RFU) $\pm$ SD of four independent experiments (*B*). Asterisks indicate statistically significant differences at $^*P < 0.05$ and $^{***}P < 0.001$.

as the biochemical hallmark of cystinosis, may not be obligatory for the dysregulation of autophagy.

While small fluctuations in the steady-state concentrations of ROS may play a role in intracellular signalling (Cadenas, 2004; Valko *et al.* 2007), uncontrolled production of ROS can lead to the expression of genes primarily controlled by redox-sensitive transcription factors. In the present study, CTNS knockdown cells had increased levels of the phosphorylated NF-κB(p65) subunit. It was previously reported that overexpressing the transcription factor NF-κB in renal proximal tubular cells increased the levels of antioxidative enzymes (George *et al.* 2012), indicating that NF-κB plays a direct role in cellular antioxidant homeostasis. Although the activity of NF-κB is principally regulated by the IκB proteins (also known as the canonical pathway) (Gilmore, 2006), NF-κB may be activated by the phosphorylation of its p65 subunit which augments its transcriptional activity (Janssen-Heininger *et al.* 2000; Gilmore, 2006), an event that occurs independently of IκB. Therefore, the phosphorylation of p65 may represent a non-canonical pathway for the activation of NF-κB. Although there is no direct evidence herein demonstrating that increased levels of ROS augmented the phosphorylation of NF-κB, it has been reported that mechanisms exist for direct and indirect activation of NF-κB by redox-sensitive enzymes (Flohé *et al.* 1997; Kabe *et al.* 2005; Pantano *et al.* 2006). Furthermore, ROS-mediated NF-κB activation is likely to depend on the type of ROS involved and as well as the cell type under investigation (Janssen-Heininger *et al.* 2000).

NRF2 represents an important stress-responsive transcription factor which interacts with the *cis*-acting elements in DNA termed antioxidant response elements (ARE) (Nguyen *et al.* 2009). These elements control the expression of genes involved in the detoxification and elimination of ROS (Nguyen *et al.* 2009). Interestingly, in the present study, CTNS knockdown cells displayed an increase in NRF2 levels. However, the unaltered generalized OS index in CTNS knockdown cells suggests an alternative mechanism for the activation of NRF2. Activation of NRF2 can occur at the level of endosplasmic reticulum (ER) through a redox-independent pathway (Cullinan *et al.* 2003; Ho *et al.* 2005). Interestingly, microarray and ultrastructural analyses of cystinotic specimens have suggested a strong link between NRF2 upregulation and ER stress in cystinosis (Sansanwal *et al.* 2010*a*). Most recently, Johnson *et al.* (2013) showed a marked ER expansion and an increase in unfolded protein response-induced chaperones Grp78 and Grp94 in *Ctns*$^{-/-}$ PTECs, a hallmark of ER stress. The authors also suggested that ER stress may influence the intracellular Ca^{2+} levels in cystinotic cells. The increased Ca^{2+} influx following CTNS knockdown observed in the present study may be a consequence of ER stress. Therefore, it can be speculated that NRF2 activation in cystinosis may be mediated by perturbations in ER homeostasis in an attempt to rescue the cells from inappropriate apoptosis.

HSPs play a role as molecular chaperones to prevent protein misfolding during and after exposure to oxidative insults (Kalmar & Greensmith, 2009). The induction of HSP32 and HSP70 in the absence of OS may suggest an involvement of a signalling pathway independent of redox perturbation. It has been suggested that HSP32 is highly specialized to sense stress conditions even at low levels, in which protein folding is compromised (Kalmar & Greensmith, 2009). Arguably, it is possible that in the present study, the redox perturbations resulting from lysosomal cystine accumulation were transient and/or below detection limits that may be sufficient to trigger HSP induction. Furthermore, the compromised antioxidant capacity in CTNS knockdown cells suggests the presence of early-phase redox perturbations in these cells.

Cysteamine has revolutionized the treatment and management of cystinosis patients by retarding both renal and non-renal complications (Gahl *et al.* 2002). However, the mechanisms of protection by cysteamine have not been fully elucidated. In the present study, cysteamine reversed the various biochemical alterations observed in CTNS knockdown cells such as reduced intracellular GSH and ATP content, decreased antioxidant capacity and augmented apoptosis. It is possible that the cysteine-boosting effect of cysteamine, being an aminothiol, may have enhanced the antioxidant capacity of kidney PTECs by promoting GSH synthesis. Indeed, we observed a marked increase in the cysteine levels in HK-2 cells following CTNS knockdown (results not shown). In agreement with our findings, Bellomo *et al.* (2010) showed that GSH levels and GSH redox status of cystinotic ciPTECs normalized following cysteamine treatment. Therefore, cytoprotective effects that cysteamine affords may be attributed to its antioxidant capacity, which can rescue the cells from the damaging effects of reactive molecules such as ROS and reactive nitrogen species.

How do these findings reconcile with the current understanding of the pathogenesis of cystinosis? The homeostatic modulation of ROS is a highly efficient mechanism allowing cells to tightly control their redox status within a very narrow range (Finkel, 2003; Cadenas, 2004; Valko *et al.* 2007). While small fluctuations in the steady-state levels of ROS may play a role in intracellular signalling (Cadenas, 2004), an uncontrolled increase in these oxidants, especially under conditions of high metabolic activity, can lead to induction of protective genes for subverting 'danger signals' and may determine cell fate. Cystinotic cells may be disadvantaged because they are more vulnerable to oxidative insults than healthy cells. Indeed, Vaisbich *et al.* (2011) reported increased levels of serum thiobarbituric acid reactive substances (TBAR) in patients with nephropathic cystinosis, which is a direct

evidence of OS in cystinosis. Therefore, cystinotic cells and tissues may be more vulnerable to oxidative insult than estimated *in vitro* and may warrant the need for antioxidant therapy to retard organ demise.

Overall, our results have demonstrated that lysosomal cystine accumulation in kidney PTECs, as a consequence of CTNS gene inhibition, promotes perturbation of cellular redox status, compromised mitochondrial function and augmented cell death. The apparent upregulation of classical stress-responsive and cytoprotective proteins and the reduction in antioxidant capacity suggest that significant disruption in redox balance initiated by lysosomal sequestration of cystine may be involved in the kidney proximal tubular dysfunction associated with cystinosis. Further studies of stress response proteins and their associated signalling pathways may offer critical insights into the important events leading to renal injury and cell death in cystinosis. This may offer novel links for targeted therapy of the disease, in combination with the cystine-depleting therapies, which can potentially lead to the attenuation of renal injury and preservation of the functions of other tissues and organs affected in cystinosis. However, it is not clear whether 'acute' *in vitro* models of cystine accumulation reflect the molecular alterations associated with the chronic cystine accumulation in cystinosis *in vivo*. To add to this complexity, there is accumulating evidence suggesting that cystine accumulation alone is not obligatory for the manifestation of molecular and physiological alterations in cystinosis (Wilmer *et al.* 2010*a*). The use of animal models that can reproduce the clinical phenotype in cystinosis, such as the $Ctns^{-/-}$ mouse (Nevo *et al.* 2010), will be hugely beneficial in shedding light into the molecular events that ultimately lead to renal injury in cystinosis.

References

Baker MA, Cerniglia GJ & Zaman A (1990). Microtiter plate assay for the measurement of glutathione and glutathione disulfide in large numbers of biological samples. *Anal Biochem* **190**, 360–365.

Bellomo F, Corallini S, Pastore A, Palma A, Laurenzi C, Emma F & Taranta A (2010). Modulation of CTNS gene expression by intracellular thiols. *Free Radic Biol Med* **48**, 865–872.

Beltowski J, Marciniak A, Jamroz-Wiśniewska A & Borkowska E (2004). Nitric oxide–superoxide cooperation in the regulation of renal Na^+K^+ATPase. *Acta Biochim Pol* **51**, 933–942.

Cadenas E (2004). Mitochondrial free radical production and cell signaling. *Mol Aspects Med* **25**, 17–26.

Chol M, Nevo N, Cherqui S, Antignac C & Rustin P (2004). Glutathione precursors replenish decreased glutathione pool in cystinotic cell lines. *Biochem Biophys Res Commun* **324**, 231–235.

Cullinan SB, Zhang D, Hannink M, Arvisais E, Kaufman RJ & Diehl JA (2003). Nrf2 is a direct PERK substrate and effector of PERK-dependent cell survival. *Mol Cell Biol* **23**, 7198–7209.

Danpure C, Jennings P & Fyfe D (1986). Further studies on the effect of chloroquine on the uptake, metabolism and intracellular translocation of [^{35}S] cystine in cystinotic fibroblasts. *Biochim Biophys Acta* **885**, 256–265.

Feliubadaló L, Font M, Purroy J, Rousaud F, Estivill X, Nunes V, Golomb E, Centola M, Aksentijevich I & Kreiss Y (1999). Non-type I cystinuria caused by mutations in SLC7A9, encoding a subunit ($b^{0,+}$AT) of rBAT. *Nat Genet* **23**, 52–57.

Finkel T (2003). Oxidant signals and oxidative stress. *Curr Opin Cell Biol* **15**, 247–254.

Flohé L, Brigelius-Flohé R, Saliou C, Traber MG & Packer L (1997). Redox regulation of NF-κB activation. *Free Radic Biol Med* **22**, 1115–1126.

Gahl W, Bashan N, Tietze F, Bernardini I & Schulman J (1982). Cystine transport is defective in isolated leukocyte lysosomes from patients with cystinosis. *Science* **217**, 1263–1265.

Gahl W, Thoene JG, Schneider JA (2001). Cystinosis: a disorder of lysosomal membrane transport. In *The Metabolic and Molecular Bases of Inherited Disease, 8 edn*, ed. Scriver CRBA, Sly WS, Valle D, Vogelstein B, pp. 5085–5108. McGraw-Hill, New York.

Gahl WA, Thoene JG & Schneider JA (2002). Cystinosis. *N Engl J Med* **347**, 111–121.

Gahl WA, Tietze F, Bashan N, Steinherz R & Schulman J (1982). Defective cystine exodus from isolated lysosome-rich fractions of cystinotic leucocytes. *J Biol Chem* **257**, 9570–9575.

George LE, Lokhandwala MF & Asghar M (2012). Novel role of NF-κB-p65 in antioxidant homeostasis in human kidney-2 cells. *Am J Physiol Renal Physiol* **302**, F1440–F1446.

Gilmore T (2006). Introduction to NF-κB: players, pathways, perspectives. *Oncogene* **25**, 6680–6684.

Gwinner W, Deters-Evers U, Brandes RP, Kubat B, Koch KM, Pape M & Olbricht CJ (1998). Antioxidant–oxidant balance in the glomerulus and proximal tubule of the rat kidney. *J Physiol* **509**, 599–606.

Han D, Canali R, Rettori D & Kaplowitz N (2003). Effect of glutathione depletion on sites and topology of superoxide and hydrogen peroxide production in mitochondria. *Mol Pharmacol* **64**, 1136–1144.

Ho HK, White CC, Fernandez C, Fausto N, Kavanagh TJ, Nelson SD & Bruschi SA (2005). Nrf2 activation involves an oxidative-stress independent pathway in tetrafluoroethylcysteine-induced cytotoxicity. *Toxicol Sci* **86**, 354–364.

Jakubowski W & Bartosz G (2000). 2, 7-dichlorofluorescin oxidation and reactive oxygen species: what does it measure? *Cell Biol Int* **24**, 757–760.

Janssen-Heininger Y, Poynter ME & Baeuerle PA (2000). Recent advances towards understanding redox mechanisms in the activation of nuclear factor κB. *Free Radic Biol Med* **28**, 1317.

Jiang F, Zhang Y & Dusting GJ (2011). NADPH oxidase-mediated redox signaling: roles in cellular stress response, stress tolerance, and tissue repair. *Pharmacol Rev* **63**, 218–242.

Johnson JL, Napolitano G, Monfregola J, Rocca CJ, Cherqui S & Catz SD (2013). Upregulation of the rab27a-dependent trafficking and secretory mechanisms improves lysosomal transport, alleviates endoplasmic reticulum stress, and reduces lysosome overload in cystinosis. *Mol Cell Biol* **33**, 2950–2962.

Kabe Y, Ando K, Hirao S, Yoshida M & Handa H (2005). Redox regulation of NF-κB activation: distinct redox regulation between the cytoplasm and the nucleus. *Antioxid Redox Signal* **7**, 395–403.

Kalatzis V, Cherqui S, Antignac C & Gasnier B (2001). Cystinosin, the protein defective in cystinosis, is a H^+-driven lysosomal cystine transporter. *EMBO J* **20**, 5940–5949.

Kalatzis V, Nevo N, Cherqui S, Gasnier B & Antignac C (2004). Molecular pathogenesis of cystinosis: effect of CTNS mutations on the transport activity and subcellular localization of cystinosin. *Hum Mol Genet* **13**, 1361–1371.

Kalmar B & Greensmith L (2009). Induction of heat shock proteins for protection against oxidative stress. *Adv Drug Deliv Rev* **61**, 310–318.

Kohen R & Nyska A (2002). Invited review: Oxidation of biological systems: oxidative stress phenomena, antioxidants, redox reactions, and methods for their quantification. *Toxicol Pathol* **30**, 620–650.

Kojima H, Urano Y, Kikuchi K, Higuchi T, Hirata Y & Nagano T (1999). Fluorescent indicators for imaging nitric oxide production. *Angew Chem Int Ed Engl* **38**, 3209–3212.

Koopman G, Reutelingsperger C, Kuijten G, Keehnen R, Pals S & Van Oers M (1994). Annexin V for flow cytometric detection of phosphatidylserine expression on B cells undergoing apoptosis. *Blood* **84**, 1415–1420.

Kregel KC (2002). Invited review: heat shock proteins: modifying factors in physiological stress responses and acquired thermotolerance. *J Appl Physiol* **92**, 2177–2186.

Laube GF, Shah V, Stewart VC, Hargreaves IP, Haq MR, Heales SJR & van't Hoff WG (2006). Glutathione depletion and increased apoptosis rate in human cystinotic proximal tubular cells. *Pediatr Nephrol* **21**, 503–509.

Levtchenko EN, Wilmer MJG, Janssen AJM, Koenderink JB, Visch HJ, Willems PHGM, de Graaf-Hess A, Blom HJ, van Den Heuvel LP & Monnens LA (2006). Decreased intracellular ATP content and intact mitochondrial energy generating capacity in human cystinotic fibroblasts. *Pediatr Res* **59**, 287–292.

Liu J, Kennedy DJ, Yan Y & Shapiro JI (2012). Reactive oxygen species modulation of Na/K-ATPase regulates fibrosis and renal proximal tubular sodium handling. *Int J Nephrol* **2012**, 1–14.

Nevo N, Chol M, Bailleux A, Kalatzis V, Morisset L, Devuyst O, Gubler MC & Antignac C (2010). Renal phenotype of the cystinosis mouse model is dependent upon genetic background. *Nephrol Dial Transplant* **25**, 1059–1066.

Nguyen T, Nioi P & Pickett CB (2009). The Nrf2-antioxidant response element signaling pathway and its activation by oxidative stress. *J Biol Chem* **284**, 13291–13295.

Nohl H & Gille L (2005). Lysosomal ROS formation. *Redox Report* **10**, 199–205.

Pantano C, Reynaert NL, Vliet AVD & Janssen-Heininger YMW (2006). Redox-sensitive kinases of the nuclear factor-κB signaling pathway. *Antioxid Redox Signal* **8**, 1791–1806.

Park M, Helip-Wooley A & Thoene J (2002). Lysosomal cystine storage augments apoptosis in cultured human fibroblasts and renal tubular epithelial cells. *J Am Soc Nephrol* **13**, 2878–2887.

Pras E, Raben N, Golomb E, Arber N, Aksentijevich I, Schapiro JM, Harel D, Katz G, Liberman U & Pras M (1995). Mutations in the SLC3A1 transporter gene in cystinuria. *Am J Hum Genet* **56**, 1297–1303.

Riccardi C & Nicoletti I (2006). Analysis of apoptosis by propidium iodide staining and flow cytometry. *Nat Protoc* **1**, 1458–1461.

Sansanwal P, Li L, Hsieh SC & Sarwal MM (2010*a*). Insights into novel cellular injury mechanisms by gene expression profiling in nephropathic cystinosis. *J Inherit Metab Dis* **33**, 775–786.

Sansanwal P, Yen B, Gahl WA, Ma Y, Ying L, Wong LJC & Sarwal MM (2010*b*). Mitochondrial autophagy promotes cellular injury in nephropathic cystinosis. *J Am Soc Nephrol* **21**, 272–283.

Schneider JA, Bradley K & Seegmiller J (1967). Increased cystine in leukocytes from individuals homozygous and heterozygous for cystinosis. *Science* **157**, 1321–1322.

Schulman J, Bradley K & Seegmiller J (1969). Cystine: compartmentalization within lysosomes in cystinotic leukocytes. *Science* **166**, 1152.

Sumayao R, McEvoy B, Martin Martin N, McMorrow T & Newsholme P (2013). Cystine dimethylester loading promotes oxidative stress and a reduction in ATP independent of lysosomal cystine accumulation in a human proximal tubular epithelial cell line. *Exp Physiol* **98**, 1505–1517.

Thoene JG & Lemons R (1980). Modulation of the intracellular cystine content of cystinotic fibroblasts by extracellular albumin. *Pediatr Res* **14**, 785–787.

Town M, Jean G, Cherqui S, Attard M, Forestier L, Whitmore SA, Callen DF, Gribouval O, Broyer M & Bates GP (1998). A novel gene encoding an integral membrane protein is mutated in nephropathic cystinosis. *Nat Genet* **18**, 319–324.

Turrens JF (2003). Mitochondrial formation of reactive oxygen species. *J Physiol* **552**, 335–344.

Vaisbich M, Guimaraes LP, Shimizu MM & Seguro AC (2011). Oxidative stress in cystinosis patients. *Nephron Extra* **1**, 73–77.

Valko M, Leibfritz D, Moncol J, Cronin MTD, Mazur M & Telser J (2007). Free radicals and antioxidants in normal physiological functions and human disease. *Int J Biochem Cell Biol* **39**, 44–84.

Vermes I, Haanen C, Steffens-Nakken H & Reutellingsperger C (1995). A novel assay for apoptosis flow cytometric detection of phosphatidylserine expression on early apoptotic cells using fluorescein labelled annexin V. *J Immunol Methods* **184**, 39–51.

Wilmer MJ, Emma F & Levtchenko EN (2010). The pathogenesis of cystinosis: mechanisms beyond cystine accumulation. *Am J Physiol Renal Physiol* **299**, F905–F916.

Wilmer MJ, Kluijtmans LA, van der Velden TJ, Willems PH, Scheffer PG, Masereeuw R, Monnens LA, van den Heuvel LP & Levtchenko EN (2011). Cysteamine restores glutathione redox status in cultured cystinotic proximal tubular epithelial cells. *Biochim Biophys Acta* **1812**, 643–651.

Wilmer MJG, de Graaf-Hess A, Blom HJ, Dijkman HBPM, Monnens LA, van den Heuvel LP & Levtchenko EN (2005). Elevated oxidized glutathione in cystinotic proximal tubular epithelial cells. *Biochem Biophys Res Commun* **337**, 610–614.

Zhao H, Kalivendi S, Zhang H, Joseph J, Nithipatikom K, Vásquez-Vivar J & Kalyanaraman B (2003). Superoxide reacts with hydroethidine but forms a fluorescent product that is distinctly different from ethidium: potential implications in intracellular fluorescence detection of superoxide. *Free Radic Biol Med* **34**, 1359–1368.

Additional information

Competing Interests

None declared.

Author contributions

R.S., with contribution from B.M., performed all experiments. R.S., T.M. and P.N. designed the study and all authors participated in the interpretation of the results. All authors contributed to writing the manuscript and to subsequent revisions.

Funding

This study was supported by the Cystinosis Foundation Ireland and the Cystinosis Research Foundation.

Acknowledgements

We gratefully acknowledge Dr Craig Slattery and the members of the UCD Renal Disease Research Group for their technical assistance and scientific discussions.